International Conference on Nuclear Data for Science and Technology 2007
DOI: 10.1051/ndata:07140

An interpretation of energy-dependence of the delayed neutron yields in the MeV-region

Takaaki Ohsawa[a] and Yoshiki Fukuda

School of Science and Engineering, Kinki University, Kowakae, Higashi-osaka 577-8502, Japan

Abstract. The steep decrease in the delayed neutron yield (DNY) in the 4- to 7-MeV region has not yet been fully understood. In the present study, an attempt was made to understand the variation in terms of increased neutron emission from fission fragments for U-235. As the incident energy increases, the excitation energy of the primary fragments increases, thus the fragments have a chance to emit more prompt neutrons. This results in decreased yields of precursors, since some of the "*would-be* precursor" fragments fail to be actual precursors after neutron emission. This process was followed nuclide-wise to obtain the final precursor yields. The initial total excitation energies (TXE) of the *would-be* precursor fragments were calculated by two methods; Case A: energy balance between total energy release and total kinetic energy (TKE) of fragments, and case B: prompt neutron multiplicity and kinetic energy. The DNYs were calculated for the two cases, using three different data for neutron separation (binding) energies: the empirical data of Audi et al., FRDM and TUYY atomic massa formulas. The results indicate that the variation of DNY is dependent on the assumtion used to estimate the initial excitation energy as well as the data set of the neutron separation energy.

1 Introduction

There are two kinds of energy dependences in the delayed neutron yields (DNY) as a function of the incident neutron energy: a) a slight decrease of DNY in the epi-thermal and resonance regions and b) a rapid decrease in the region from 4 to 7 MeV. One of the authors [1,2] indicated a possibility of fluctuations (local dips for U-235) in the DNY at resonances on the basis of the multimodal random neck-rupture model [3] and on the experimental measurements performed by Hambsch [4,5] at IRMM, and this may explain the slight decrease in DNY in the resonance region. As for phenomenon (b), Alexander et al. [6] interpreted it as partially due to energy-dependent even-odd effect in the fission yield.

The present authors examined another hypothesis that increased successive neutron emission from highly-excited primary fission fragment for higher incident neutron energies leads to loss of precursors at higher incident neutron energy.

2 Method

2.1 Summation calculation

The total DN yield was calculated using the summation method:

$$\nu_{\mathrm{d}} = \sum_i Y_i P_{ni}, \tag{1}$$

where Y_i is the post-neutron-emission fission yield and P_{ni} is the DN emission probability of precursor i. The evaluated data for the DN emission probability P_{ni} were taken from Wahl [7], because this set comprises largest number (271) of precursors.

The post-neutron-emission fission yield Y_i was calculated starting from the pre-neutron-emission fission yields of precursors and their initial excitation energies. The pre-neutron-emission fission yields were calculated with the five-Gaussian representation of fragment mass distribution of Knitter et al. [8] and Hambsch et al. [9] and the fragment charge distribution of Gaussian shape with standard deviation σ = 0.56 and the most probable charge

$$Z_{\mathrm{p}} = Z_{\mathrm{UCD}} \pm \delta Z, \tag{2}$$

where Z_{UCD} is the charge predicted with the UCD (unchanged charge distribution) hypothesis. The deviation δZ from the UCD hypothesis is known to be undulating around 0.5, the plus sign referring to light fragments and minus sign to heavy fragments, respectively. Considering that a small change in Z_{p} causes large differences in fission yield calculations, we took into account these undulations [7] in the present calculations. The isomer production ratios were calculated according to the prescription of Madland et al. [10].

2.2 Initial excitation energies

The initial total excitation energies (TXE) and its partition between the two primary fission fragments were calculated according to two methods: energy balance between total energy release and total kinetic energy (TKE) of fragments, and prompt neutron multiplicity and kinetic energy.

A. Energy balance method

In this method, $TXE(E_{\mathrm{n}})$ was calculated with the energy balance equation

$$TXE(E_{\mathrm{n}}, A) = E_{\mathrm{r}}(A) + B_{\mathrm{n}}(A) + E_{\mathrm{n}} - TKE(E_{\mathrm{n}}, A). \tag{3}$$

The total energy release E_{r} of fission was calculated using the TUYY mass formula [11], and the neutron binding energy

[a] Presenting author, e-mail: ohsawa@ele.kindai.ac.jp

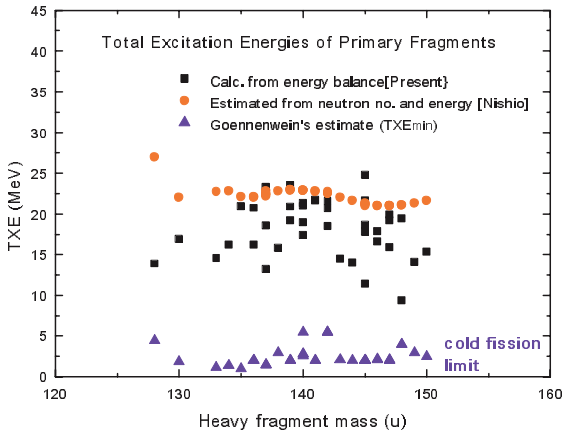

Fig. 1. TXEs of primary fragments calculated from energy balance, equation (3), and from neutron multiplicity and kinetic energy [12]. Note that present calculation refers to specific fragments leading to precursors after neutron emission. The minimum TXEs reported by Gönnenwein [14,15], corresponding to "cold fission", are also shown.

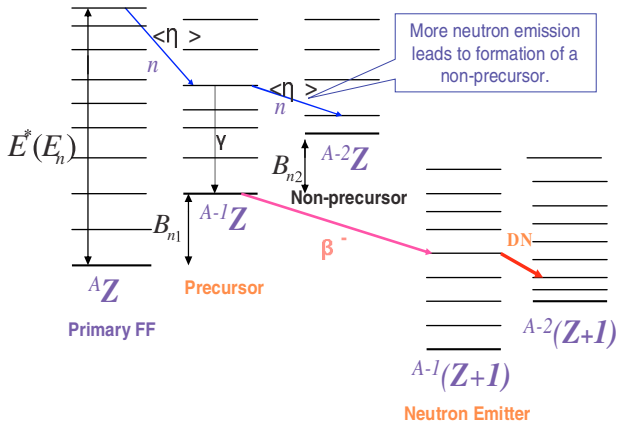

Fig. 2. Nuclear transmutation of fission fragments by neutron emission and beta-decay. At higher initial energies $E^*(E_n)$, increased neutron emission leads to loss of yield of precursors.

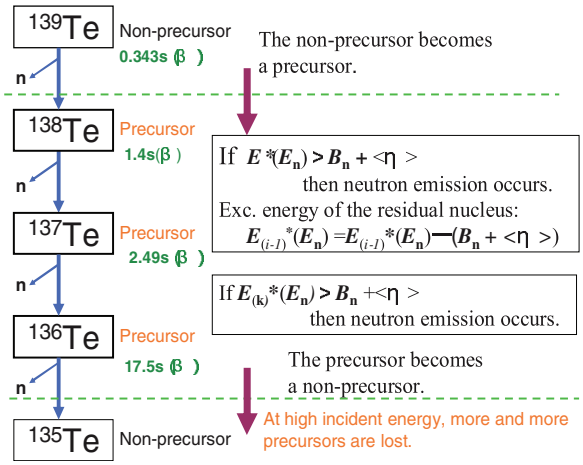

Fig. 3. Nuclear transmutation of tellurium isotopes by neutron emission.

B_n for U-236 is 6.546 MeV. The measurement of TKE as a function of the incident neutron energy E_n by Hambsch et al. [8] for $E_n = 0$ up to 5.5 MeV was used, and the experimental data of TKE as a function of fragment mass A by Knitter et al. [9] was adopted in the present calculation. It was assumed that equipartition law of energy is valid, thus the excitation energy is proportional to the mass number of the fragment.

B. Prompt neutron method

The TXE can also be estimated from the multiplicity and kinetic energy of prompt neutrons emitted from each fragment. The TXE is the sum of excitation energies of the two fragments:

$$TXE(A_{\rm L}, A_{\rm H}) = E^*(A_{\rm L}) + E^*(A_{\rm H}). \quad (4)$$

The excitation energies in turn were calculated with the following relation:

$$E^*(A) = \nu(A)[\eta(A) + B_{\rm n}(A)] + B_{\rm n}(A)/2, \quad (5)$$

where $\nu(A)$ and $\eta(A)$ are the average number and the fragment center-of-mass kinetic energy of prompt neutrons, respectively, and $B_{\rm n}(A)$ the neutron binding energy for a fragment with mass number A. Nishio [12] calculated the TXE using his measured data of ν(A) and $\eta(A)$. In the present analysis $\eta(A)$=1.33 MeV was used, although the quantity $\eta(A)$ varies slightly as a function of A. The partition of TXE between the light and heavy fragments was calculated based on Terrel's scission point model [13]. The deformation energy $E_{{\rm def},i}$ and fragment deformation parameters α_i are expressed as follows:

$$E_{{\rm def},i} = V_{\rm c}^2/(4\alpha_i Z_{\rm L}^2 Z_{\rm H}^2) \quad (6)$$

$$\alpha_i = \alpha_{0,i}(0.5 - \delta W)/(0.5 + \delta W) \quad (7)$$

$$\alpha_{0,i} = 2.86 - 0.0630\, Z_i^2/A, \quad (8)$$

where $V_{\rm c}$ is the Coulomb potential energy which in turn was assumed to be equal to TKE. The quantity δW stands for the shell correction energy. Equation (8) assumes the liquid drop model. Hence, we have

$$E_{{\rm def},1}/E_{{\rm def},2} = \alpha_2/\alpha_1. \quad (9)$$

The TXEs calculated by the two methods are shown in figure 1. It can be seen that there is a considerable difference between the two calculations. For comparison, in the figure we show the minimum TXEs corresponding to "cold fission" [14,15].

2.3 Nuclear transmutation by neutron emission before beta-decay

Primary fission fragments with high excitation energies decay by neutron emission. Some fragments decay into DN

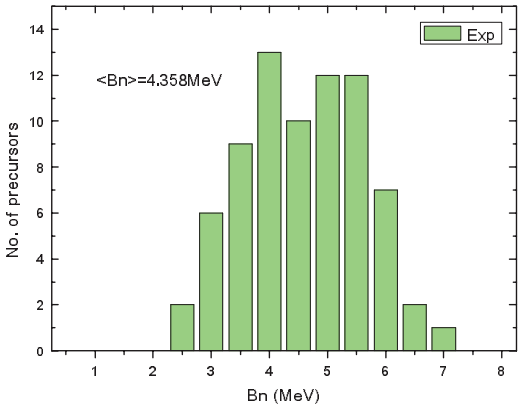

Fig. 4 (a). Distribution of neutron binding energies for major precursor nuclides obtained from experimental data base of Audi and Wapstra [16].

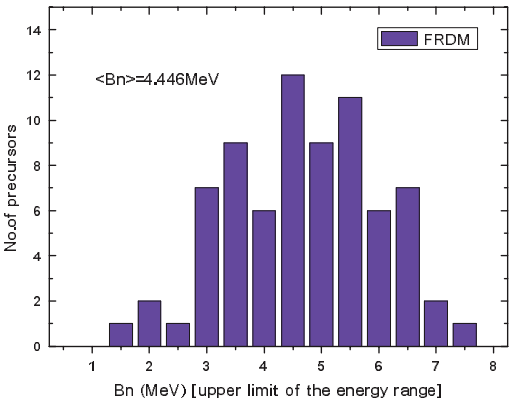

Fig. 4 (b). Distribution of neutron binding energies for major precursors calculated with FRDM formula [17].

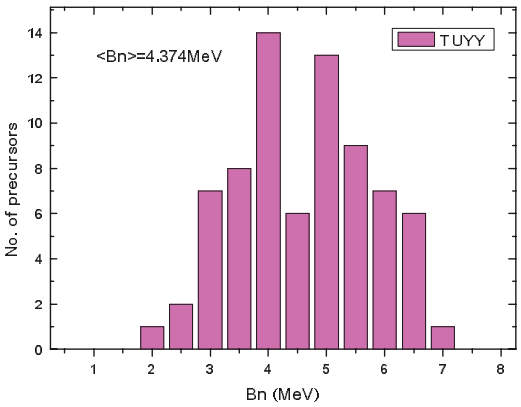

Fig. 4 (c). Distribution of neutron binding energies for major precursors calculated with TUYY formula [11].

precursors. However at higher incident neutron energies, the primary fragments are highly excited, thus the fragments have more chance to emit more prompt neutrons. This results in decreased yields of precursors, since some of the "*would-be* precursor" nuclides fail to be actual precursors after neutron emission (fig. 2). On the other hand, some neutron-rich fragments that terminated before arriving at precursor nuclides in

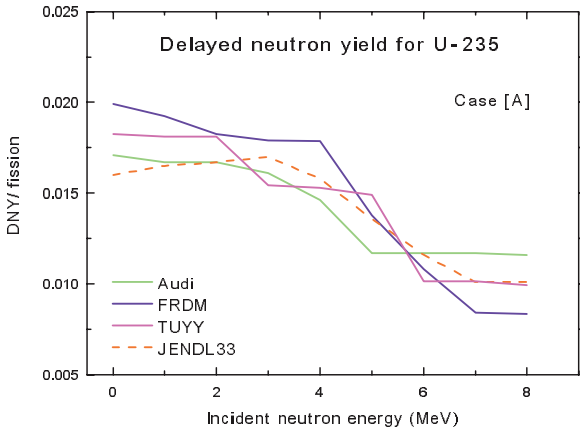

Fig. 5 (a). DNY as a function of incident neutron energy for case A.

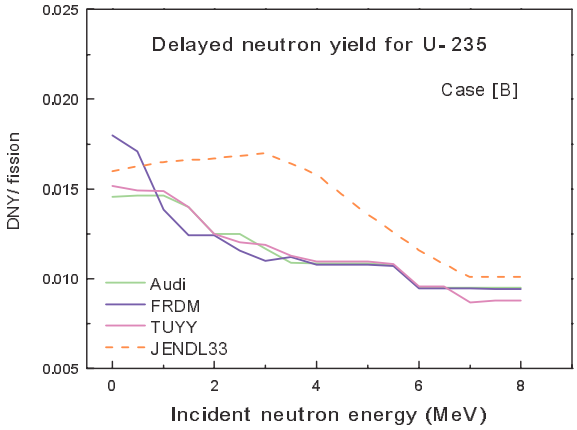

Fig. 5 (b). DNY as a function of incident neutron energy for case B.

the process of neutron emission, can reach precursors at higher incident energies. This results in increased yields of precursors (fig. 3).

However, the latter effect is smaller than the former, since the fission yield of the more neutron-rich fragments are generally smaller than the less neutron-rich fragments. Thus, the overall yield of precursors is supposed to decrease as a function of the incident energy. In order to verify this inference, we followed the neutron-emission process nuclide (precursor)-wise from its initial state until last neutron emission to obtain the final fission yield of precursors. The fission yields of the primary fission fragments were calculated by multimodal random- neck-rupture model with parameters obtained by Hambsch [9]. The neutron binding energies were obtained from empirical data of Audi and Wapstra [16], FRDM [17] and TUYY [11] atomic mass formulas. The frequency distribution of neutron binding energies for major precursors with the energy bin of 0.5 MeV are shown in figures 4 (a), (b) and (c). There is almost no difference in the average value $\langle B_n \rangle$, but there is a considerable difference the distribution. This will bring about a difference in the neutron emission process of precursor nuclides.

3 Results and discussion

The results of calculation of the DNY as a function of incident neutron energy E_n for case A and B are shown in figures 5 (a) and (b).

Comparing the calculations with JENDL-3.3 evaluation, shown with a dashed line, we see that the calculated DNY for case A decreases rapidly in the region 3 to 7 MeV, in better agreement with the evaluation than in case B. The difference observed in the DNY for the three sets of neutron binding energies is due to different distribution of values as shown in figures 4 (c)(a)–(c), because the rate of subsequent neutron emission process of figure 3 is determined by the neutron binding energies of the fission fragments.

The reason for considerable difference between cases A and B lies in the difference in the initial TXE for primary fission fragments. Higher TXE of case B leads to a longer chain of neutron emission, thus to faster loss of precursors. In contrast, lower TXE of case A results in slower loss of precursors, followed by a rather steep drop at higher incident energies. As suggested by lower limit of TXE [14, 15] for the case of "cold fission", the actual TXE is considered to be distributed between the higher and lower limits. It should be mentioned here that, in the present analysis, only average behaviour was considered, i.e., the TXE and prompt neutron kinetic energy was represented by their average values. Thus, in order to be more accurate, it is important to consider the neutron emission process with proper distribution of these quantities.

References

1. T. Ohsawa, T. Miura, J. Nucl. Sci. Technol. Suppl. **2**, 100 (2002).
2. T. Ohsawa, F.-J. Hambsch, Nucl. Sci. Eng. **148**, 50 (2004).
3. U. Brosa, S. Grossmann, A. Müller, Physics Reports **197**(4), 167 (1990).
4. F.-J. Hambsch, H.-H. Knitter, C. Budtz-Jørgensen, Nucl. Phys. A **491**, 56 (1989).
5. F.-J. Hambsch, L. Dematté, H. Bax, I. Ruskov, J. Nucl. Sci. Technol. Suppl. **2**, 307 (2002).
6. D.R. Alexander, M.S. Krick, Nucl. Sci. Eng. **62**, 627 (1977).
7. A.C. Wahl, At. Nucl. Data Tables **39**, 1 (1988).
8. H.-H. Knitter, F.-J. Hambsch, C. Budtz-Jøregnsen, J.P. Theobald, Z. Naturforsch. **42a**, 786 (1987).
9. F.-J. Hambsch et al. (2005) (private communication).
10. D.G. Madland, T.R. England, Nucl. Sci. Eng. **64**, 859 (1977).
11. T. Tachibana et al., At. Nucl. Data Tables **39**, 251 (1988).
12. K. Nishio, Ph.D. thesis, Kyoto University, 1997 (in Japanese).
13. J. Terrel, *Proc. of IAEA Symposium on Physics and Chemistry of Fission*, *Salzburg*, Vol. 1 (1965), p. 3.
14. F. Gönnenwein, B. Börsig, Nucl. Phys. A **530**, 27 (1991).
15. F. Gönnenwein, Z. Phys. A **259**, 259 (1994).
16. G. Audi, A.H. Wapstra, Nucl. Phys. A **595**, 409 (1995).
17. P. Möller, J.R. Nix, W.D. Myers, W.J. Swiatecki, At. Nucl. Data Tables **59**, 189 (1995).